organics

MDPI

Article

Unveiling the Relationship between Structure and Anticancer Properties of Permethylated Anigopreissin A: A Study with Thirteen Analogues

Ilaria Caivano [1,†], Alessandro Santarsiere [1,†], Mario Amati [1], Paolo Convertini [1], Maria Funicello [1], Paolo Lupattelli [2], Lucia Chiummiento [1,*] and Anna Santarsiero [1]

[1] Department of Science, University of Basilicata, Via dell'Ateneo Lucano, 10, 85100 Potenza, Italy; ilaria.caivano@unibas.it (I.C.); alessandro.santarsiere@unibas.it (A.S.); mario.amati@unibas.it (M.A.); paolo.convertini@gmail.com (P.C.); maria.funicello@unibas.it (M.F.); anna.santarsiero@unibas.it (A.S.)

[2] Department of Chemistry, Sapienza University of Rome, p.le Aldo Moro 5, 00185 Roma, Italy; paolo.lupattelli@uniroma1.it

* Correspondence: lucia.chiummiento@unibas.it; Tel.: +39-0971-205492; Fax: +39-0971-295678

† These authors contributed equally to this work.

Abstract: Permethylated anigopreissin A (PAA), a fully protected form of the natural anigopreissin A, was found in our previous study to be active against several cancer cells, up to IC50 0.24 μM for HepG2 cells. Herein, a total of thirteen PAA analogues with variations in the number, position of substituents and unsaturation were synthesised starting from a common precursor, and their ability to induce cell growth inhibition was tested. By comparing the antiproliferative effect of the analogues with PAA and with the help of computational studies, we have gained valuable insights into both the biological activity and structure of this natural class of compounds. Indeed, we discovered the importance of the C-3 ring in modulating the biological activity of PAA, as well as the crucial role of the *trans* configuration of the styryl double bond and the significance of substitutions on the other parts of the molecule.

Keywords: permethylated anigopreissin A; resveratrol dimer; divergent synthesis; antiproliferative effect; hepatocellular carcinoma cells

Citation: Caivano, I.; Santarsiere, A.; Amati, M.; Convertini, P.; Funicello, M.; Lupattelli, P.; Chiummiento, L.; Santarsiero, A. Unveiling the Relationship between Structure and Anticancer Properties of Permethylated Anigopreissin A: A Study with Thirteen Analogues. *Organics* **2024**, *5*, 237–251. https://doi.org/10.3390/org5030012

Academic Editor: Igor V. Trushkov

Received: 18 June 2024
Revised: 8 July 2024
Accepted: 29 July 2024
Published: 1 August 2024

1. Introduction

Stilbenoids, widely distributed in plants such as vegetables, fruits, teas, and some herbs, are recognised as essential dietary components contributing to the management of chronic inflammation [1]. Resveratrol and its oligomers, which belong to the stilbenoid class, are renowned for their diverse biological activities, encompassing anti-inflammatory, antioxidative, antimicrobial, and anticancer properties [2,3]. Several resveratrol dimers feature a benzofuran or dihydrobenzofuran core, along with a styryl moiety exhibiting either a *trans* configuration (e.g., anigopreissin A) or a *cis* configuration (e.g., ε-viniferin) [4], or an arylethyl substituent (e.g., gneafricanin D) [5]. Additionally, other dimers arise from the dimerisation of oxyresveratrol, piceatanol, or isorhapontigenin (e.g., bisisorhapontigenin B) [6] (Figure 1).

The significant interest in discovering new anticancer compounds has spurred us to advance our investigation of anigopreissin A and its analogues. Anigopreissin A, a dimer of resveratrol naturally occurring in *Anigozanthos preissi*, *Musa Cavendish* [7], and *Macropidia fuliginosa*, exhibits modest antimicrobial activity against *S. aureus* and *S. pyogenes* [8]. Furthermore, permethylated anigopreissin A [9] (PAA), representing a fully protected version of anigopreissin A, demonstrates compelling cytotoxicity against a wide spectrum of human tumour cell lines, including HepG2, MCF7, U937, and SHSY5Y.

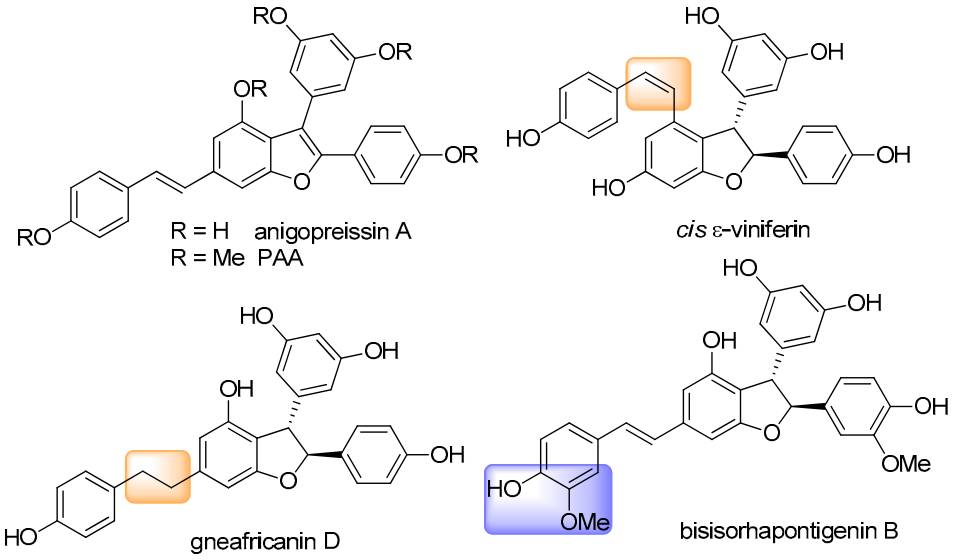

Figure 1. Examples of resveratrol dimer derivatives.

PAA triggers cancer cell death by inducing cell cycle arrest in the G1 phase, likely mediated through the cyclin E/CDK2 complex. Notably, exposure to PAA leads to an up-regulation of the CDKN1B gene, a specific inhibitor of the cyclin E/CDK2 complex [10]. The molecular mechanisms underlying the death of PAA-treated cancer cells involve the intrinsic apoptotic pathway.

Our previous studies have shown that PAA exerts the most potent antiproliferative effect on hepatocellular carcinoma cell lines, specifically HepG2 and Alexander [10]. Importantly, its cytotoxic activity is also selective towards cancer cells, as non-tumorigenic cells such as HEK293 and human fibroblasts remain unaffected by PAA. A recent study suggests that PAA induces its effect in HCC cells via GDH1 inhibition, although other molecular mechanisms could be involved [11].

Moreover, PAA demonstrated higher activity compared to trimethylated resveratrol, as well as higher activity compared to simpler structures or synthetic precursors, which exhibited either no activity or lower activity than PAA [10].

To deepen our comprehension of the structure–activity relationship of PAA and to develop more potent cytotoxic compounds, it is crucial to construct various analogues. For this objective, our primary focus was on varying the number of methoxy groups on the aryl moieties and the degree of unsaturation of the ethylene bridge within the PAA scaffold. We opted to employ the same synthetic strategy used for PAA, with modifications limited to the sequence and adoption of common precursors as advised by the diversity-oriented synthesis (DOS) methodology [12].

In this work, thirteen PAA analogues were efficiently synthesised using domino Sonogashira-heteroannulation reactions [13], olefination reactions (Wittig or Julia–Kocienski reactions), chemoselective reductions and Suzuki cross-couplings (Scheme 1). We decided to engage nearly fully permethylated derivatives since it is known that methylated resveratrol derivatives have shown a higher antiproliferative effect on cancer cells compared to their hydroxylated counterparts. This is likely due to their increased lipophilic properties that enhance uptake through the cell membrane [14] and due to the inhibition of metabolic conjugation reactions. To elucidate the structure–activity relationship of PAA, cell viability assays of all synthetised analogues were performed using PAA as the reference compound and computational studies were conducted on a selected number of analogues.

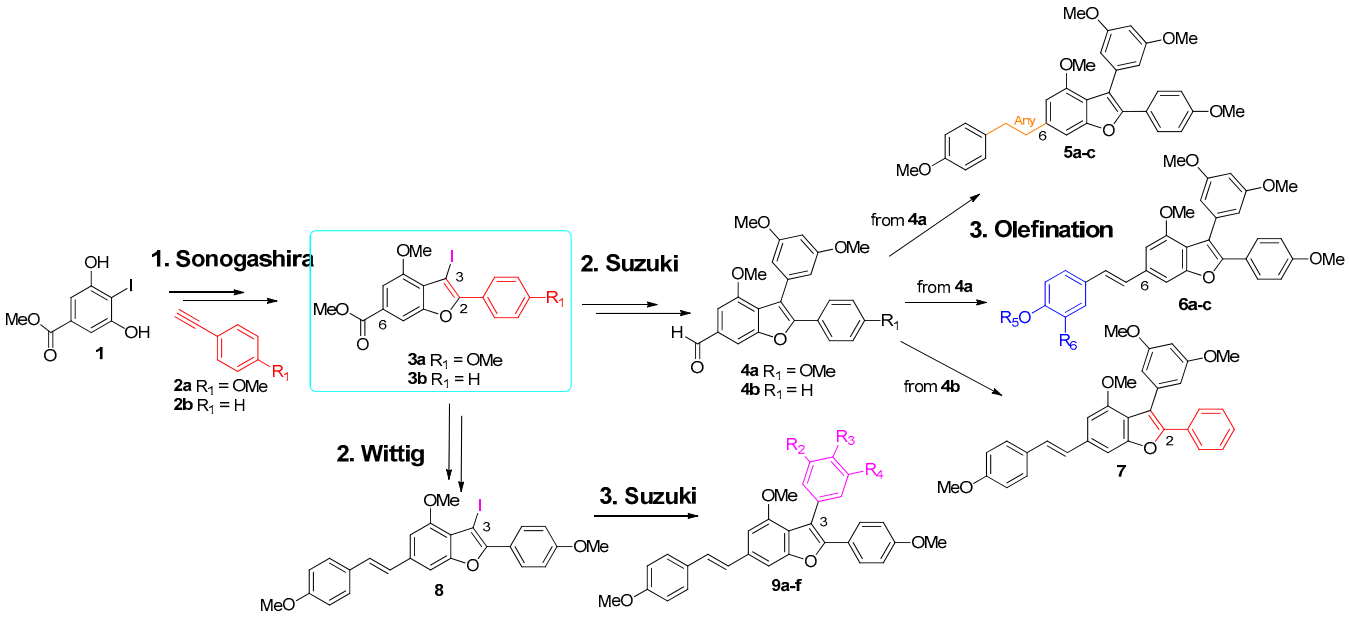

Scheme 1. General strategy to prepare derivatives **5a–c**, **6a–c**, **7** and **9a–f**.

2. Materials and Methods

2.1. General Procedures

All reagents were supplied by Sigma-Aldrich, TCI, and AlfaAesar companies and were used without further purification unless otherwise stated.. All reactions were carried out in oven-dried glassware under an argon atmosphere unless otherwise noted. Flash chromatography was performed using 60–200 mesh silica gel. ^{1}H NMR spectra were recorded on Varian 400 MHz and Varian 500 MHz spectrometers at room temperature with $CDCl_3$ as the solvent unless otherwise noted. ^{13}C NMR spectra were recorded on Varian 100 MHz and Varian 125 MHz spectrometers, all at room ambient temperature. Chemical shifts are reported in parts per million relative and referenced internally to the residual solvent resonances: ^{1}H NMR spectra to $CDCl_3$ at δ 7.26 and ^{13}C NMR spectra to $CDCl_3$ at δ 77.0. Data for ^{1}H NMR are reported as follows: chemical shift, multiplicity (s = singlet, d = doublet, t = triplet, q = quartet, and m = multiplet), coupling constants (in Hertz), and integration. Mass spectra were obtained using FT-ICR/MS by using ESI in the positive ion mode.

2.1.1. General Procedure of Wittig Olefination for the Preparation of Compound **5a**, **6b**, **6c**, **7**, and **8**

To a stirred solution of triphenyl arylphosphonium bromide **10** ((4-methoxybenzyl)triphenylphosphonium bromide) or **16** ((3,4-dimethoxybenzyl)triphenylphosphonium bromide) or **17** ((4-((*tert*-butyldimethylsilyl)oxy)-3-methoxybenzyl)triphenylphosphonium bromide) (0.85 mmol, 1.1 equiv.) in *i*-PrOH (20 mL), LiBr (0.224 g, 2.61 mmol, 3.4 equiv) and $LiOH{\cdot}H_2O$ (0.058g, 1.39 mmol, l.8 equiv) were added at room temperature. After 15 min, a solution of **4a** (3-(3,5-dimethoxyphenyl)-4-methoxy-2-(4-methoxyphenyl)benzofuran-6-carbaldehyde) or **4b** (3-(3,5-dimethoxyphenyl)-4-methoxy-2-phenylbenzofuran-6-carbaldehyde) or **34** (3-iodo-4-methoxy-2-(4-methoxyphenyl)benzofuran-6-carbaldehyde) (0.76 mmol, 1 equiv.) in *i*-PrOH (10 mL) was added to the mixture and heated to reflux. After 3 h, the mixture was quenched with H_2O and extracted with EtOAc (3 × 40 mL). The combined organic layers were dried over Na_2SO_4, filtered, and concentrated under reduced pressure. The *cis*/*trans* crude mixture of product **5a** was purified by column chromatography (petroleum ether/EtOAc 9:1), avoiding light, while the crude compounds **6b**, **6c**, **7**, and **8** were firstly isomerized with catalytic amounts of I_2 in heptane/DCM (7:3) at room temperature in the dark for one night and then purified by column chromatography.

2.1.2. Reduction of the Styryl Double Bond for Preparation of Compound **5b**

To a stirred solution of PAA (21.1 mg, 0.0404 mmol) in dry THF (0.400 mL), 2-nitrobenzensulfonyl chloride (20.3 mg, 0.0916 mmol) was added. The reaction mixture was cooled to 0 °C, and then hydrazine (16 µL, 0.326 mmol) was added. After stirring for 5 days at room temperature, the reaction mixture was quenched by dilution with AcOEt. The organic phase was washed with a saturated aqueous solution of NH_4Cl (2 × 5 mL), dried over Na_2SO_4 and concentrated under reduced pressure. The crude was purified by column chromatography on silica gel (EP/AcOEt, 9:1). Compound **5b** was isolated (11.6 mg, 55% yield) as a pale yellow solid.

2.1.3. Julia–Kocienski Reaction for Preparation of Compound **6a**

To a solution of 4-((benzo[*d*]thiazol-2-ylsulfonyl)methyl)phenyl *tert*-butyl carbonate **14** (0.121 g, 0.3 mmol) in dry THF (0.1M) at −78 °C, a solution of KHMDS in toluene (1M) (0.3 mmol) was added and the mixture was stirred for 30 min. A solution of aldehyde **4a** (0.084 g, 0.2 mmol) in THF (0.3M) was cannulated into the reaction mixture. The reaction mixture was allowed to warm to room temperature. After 8 h, it was quenched by adding a saturated aqueous solution of $NaHCO_3$ and extracted with Et_2O. The organic phases were washed with brine, dried over Na_2SO_4, and concentrated under reduced pressure. The crude mixture *cis*/*trans* of the reaction was isomerized by using a catalytic amount of I_2 in heptane/DCM 7:3 for a night. The crude mixture was then purified by column chromatography on silica gel (petroleum ether/Et_2O 8:2), affording **15** (72%, 0.088 g, 0.14 mmol) as a pale yellow solid.

2.1.4. General Procedure for the Suzuki Reaction for the Preparation of Compounds **33**, **9a**–**9f**

To a solution of iodide **3b** or **8** (1.14 mmol, 1.0 equiv.) in DMF/H_2O (4:1, 22.8 mL), aryl boronic acid (1.6 mmol, 1.4 equiv.), $NaHCO_3$ (0.133 g, 1.6 mmol), and $PdCl_2(PPh_3)_2$ (0.040 g, 0.057 mmol) were added. The solution was stirred for 10 min at room temperature and then heated at 80 °C for 7 h. After cooling, the mixture was diluted with AcOEt and washed with a saturated aqueous solution of NH_4Cl, brine, and water. The organic layer was dried over Na_2SO_4, filtered, and concentrated under reduced pressure. The crude was purified (silica gel; petroleum ether/AcOEt, 9:1) to afford the desired product **33**, or **9a**–**9f**.

2.2. Cell Culture, Treatments, and Viability Assay

HepG2 cells were cultured as previously described [11]. Alexander cells were grown in Roswell Park Memorial Institute (RPMI) 1640 Medium (Thermo Fisher Scientific, San Jose, CA, USA) supplemented with 10% foetal bovine serum, 2mM L-glutamine, 100 U/mL of penicillin, and 100 µg/mL of streptomycin at 37 °C in a humidified atmosphere containing 5% CO_2. Cells were screened periodically for mycoplasma contamination.

PAA and the thirteen analogues were dissolved in 100% dimethyl sulfoxide (DMSO) (Sigma-Aldrich, St Louis, MO, USA) and diluted in a complete culture medium to obtain a final concentration of 0.1% DMSO in the cells.

2.2.1. Cell Viability Assay

Cell viability was determined by colourimetric 3-(4,5-dimethylthiazol-2-yl)-2,5-diphenyltetrazolium bromide (MTT) assay. The cells (5×10^4) were seeded in a 96-well plate and, 24 h later, were treated with PAA or PAA analogues at increasing concentrations (10 nM, 100 nM, 1 µM, 10 µM, and 100 µM) for 72 h. The control groups received DMSO equivalent to the maximum percentage of <0.1% solvent used in the experimental settings. At the end of the treatments, an MTT assay was performed as described in [15]. The optical density was determined at 570 nm with a GloMax® Discover Microplate Reader (Promega, Madison, WI, USA).

2.2.2. Statistical Analysis

The statistical analysis was performed by GraphPad Prism software (La Jolla, CA, USA). The results are presented as mean ± standard deviation (SD) from three independent experiments with four replicates in each. Data were analysed using one-way ANOVA followed by Dunnett's multiple comparison test. The asterisks in the figures denote statistical significance (* $p < 0.05$, ** $p < 0.01$, and *** $p < 0.001$).

2.3. Computational Details

All the computations were performed with the Gaussian 09 software, version C01 [16] (G09 in the following). The M06 xc functional [17] was used in all the reported computations. The integration grid was set to the "ultrafine" level (as implemented in G09). SCF procedures and structure optimizations were performed with the default convergence thresholds as set in G09.

For the research of the most stable conformers of PAA—**9a**, **9b**, and **9c**—the 6-31G(d) basis set [18] (as implemented in G09) was used for a quicker investigation of the potential energy surface. The more accurate cc-pVTZ basis set [19] (as implemented in G09) was used for refining the structures and their electronic structures. All the data reported in Table S1 and Figures S4 and S5 were extracted from the cc-pVTZ-based computations.

The atomic charges in Table S1 (see Section S9 in Supporting Information) are Mulliken's well-known atomic charges and the natural charges obtained by the NBO-based electron density analysis, known as natural population analysis (NPA) [20]. In the last case, the NPA implementation inside G09 was used with the default options ("population npa" option).

Graphical representations of computational studies were prepared through the MolDen 5.7 program [21].

3. Results and Discussion

3.1. Synthesis of the Thirteen Analogues

As depicted in Scheme 1, the thirteen analogues were prepared using two key building blocks, **4** and **8**, synthetised alternatively by Suzuki arylation or by Wittig olefination of **3** derivatives. On these compounds, the olefination or the Suzuki reaction was performed in order to insert the desired structural motif.

3.1.1. Synthesis of Analogues **5a–c** and **6a–c**

To decipher the significance of the *trans* double bond in the PAA biological activity, we constructed the first series of analogues containing various linkages between the benzofuran portion and the *p*-methoxybenzene: a *cis* double bond (**5a**), a fully saturated bridge (**5b**), or a triple bond (**5c**). The synthesis of these new derivatives was carried out following the procedure outlined in Scheme 2. The key intermediate **4a** was prepared according to our previously reported strategy [9]. Then, it was involved in the Wittig olefination reaction with the phosphonium salt **10**, LiOH, and LiBr in *i*-PrOH to afford PAA as a mixture of *cis*/*trans* isomers in a 1:1 ratio [22]. Compound **5a**, representing the *cis* isomer of PAA, was isolated from the mixture via column chromatography. Subsequently, the *trans* isomer, PAA, was chemoselectively reduced to compound **5b** using *o*-NO_2PhCl and hydrazine hydrate in THF [23].

The derivative **5c**, featuring a triple bond, was synthesised starting from the same aldehyde **4a**, which was converted into the corresponding dibromovinyl compound **11** using PPh_3 and CBr_4 in DCM [24]. Subsequently, compound **11** was transformed into the alkyne **12** with Cs_2CO_3 in DMSO [25] at 110 °C, yielding compound **12** (50%, two steps). Compound **12** was then subjected to a Sonogashira reaction with *p*-methoxy-phenyl iodide **13**, leading to compound **5c** (40%).

The second class of compounds (**6a–6c**) was designed to assess the impact of the substituents on the styrene ring, and again, compound **4a** was the key intermediate. Among them, compound **6a** features a hydroxyl group on the aryl of the styryl moiety instead of the methoxy group found in PAA, while compounds **6b** and **6c** contain an additional methoxy

group in the *ortho* position to the hydroxyl or methoxyl group of **6a** or PAA, respectively. The analogue **6a**, bearing a free hydroxyl group, was prepared via the Julia–Kocienski olefination using the heteroaryl-sulfone **14** (Scheme 3).

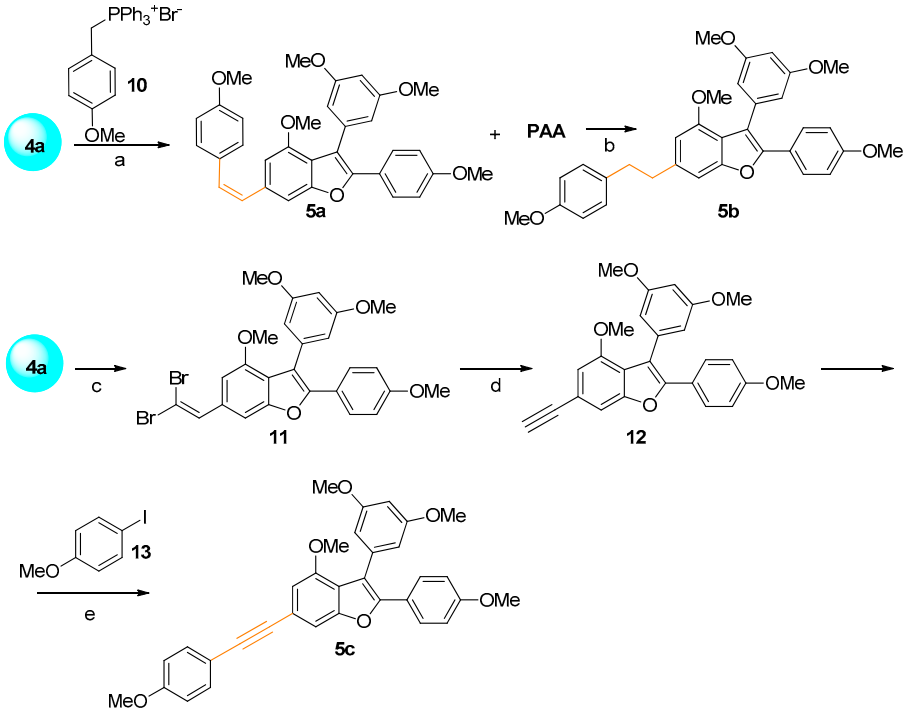

Scheme 2. (a) **10**, LiOH, LiBr, i-PrOH, reflux, 80%; (b) *o*-NO_2PhCl, $NH_2NH_2{\cdot}H_20$, THF, rt, 55%; (c) PPh_3, CBr_4, DCM, rt; (d) Cs_2CO_3, DMSO, 110 °C, 50% in two steps; (e) **13**, $PdCl_2(PPh_3)_2$, CuI, Et_3N, reflux, 40%.

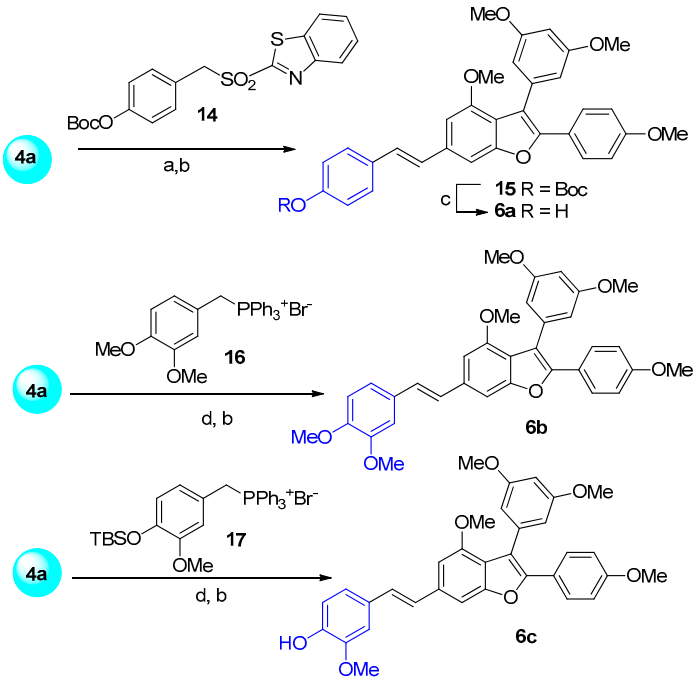

Scheme 3. (a) **14**, KHMDS, THF, −78 °C; (b) I_2 cat., *n*-heptane: DCM (7:3), 72%, 44%, and 34% in two steps for compounds **15**, **6b**, and **6c**, respectively; (c) CBr_4, PPh_3, MeOH, quant.; (d) LiOH, LiBr, *i*-PrOH.

Attempts to carry out the Wittig olefination with phosphonium salts bearing a TBS or a Boc [26] protecting group resulted in very low yields. Consequently, the Julia–Kocienski reaction was selected as the preferred olefination method. The synthesis of heteroaryl-sulfone **14** started from the commercially available aldehyde **18**, which was first protected as the Boc carbonate **19** [27] and then reduced to alcohol **20** using $NaBH_4$ [26] (as depicted in Scheme 4). The benzylic alcohol, by the corresponding tosylated [25], was converted into the sulphide during the nucleophilic substitution with mercaptobenzothiazol **21**. The obtained BT-sulphide was then oxidised quantitatively to sulfone **14** with *m*CPBA [28]. The Julia–Kocienski olefination employing KHMDS as the base furnished olefin **15** [29] as a mixture of *cis*/*trans* isomers (approximately 1:1 ratio), which was then isomerized by iodine to the *trans* isomer **15** in 72% yield. Finally, the removal of the Boc group with CBr_4 and PPh_3 in MeOH afforded compound **6a** in a quantitative yield (Scheme 3) [30].

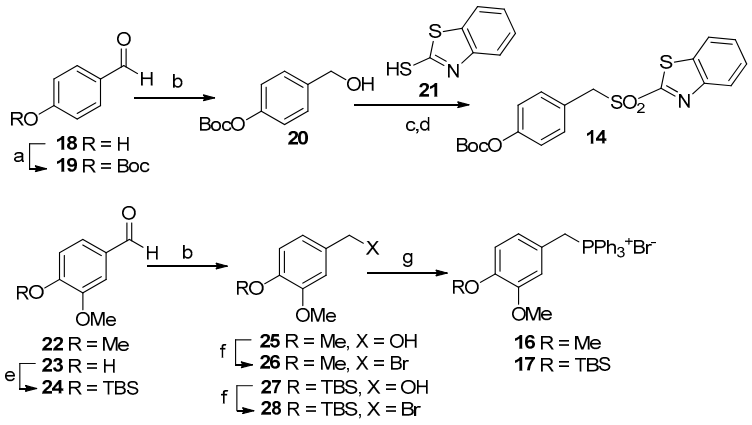

Scheme 4. (a) $(Boc)_2O$, DIPEA, DMAP, THF, 2h, rt, quant.; (b) $NaBH_4$, EtOH, 10 min, quant. for **20**, 73% for **25** and 79% in two steps for **27**; (c) TsCl, Bu_4NI, NaOH, toluene, 4h, rt, then, **21**, 2h, rt 56% in two steps; (d) *m*CPBA, DCM, 8h, rt, quant.; (e) only for aldehyde **23**, TBSCl, DMAP, DCM, 1h, rt; (f) NBS, PPh_3, DCM, 8h, 0 °C, 47% and 49% for compounds **26** and **28**, respectively; (g) PPh_3, toluene, reflux, 96% and 88% for compounds **16** and **17**.

The preparation of compounds **6b** and **6c** was performed employing the classical Wittig protocol, where phosphonium salts **16** and **17** were prepared starting from the commercially available aldehydes **22** and **23** (Scheme 4).

Aldehyde **22** was directly reduced with $NaBH_4$ to benzylic alcohol **25** [31] in a 73% yield, which was then transformed into bromide **26** using NBS and PPh_3 in DCM [32] in a 47% yield. Vanillin **23** was first protected by a TBS group and subsequently reduced to benzylic alcohol **27** [33] (a 79% yield over two steps). Alcohol **27** was then converted into bromide **28** [32] with a 49% yield. Both bromides were treated with PPh_3 in toluene to form the phosphonium salts **16** and **17** in 96% and 88% yields, respectively. The final Wittig olefination and isomerization furnished exclusively *trans* isomers of compounds **6b** (in a 44% yield over two steps) and **6c** (in a 34% yield over two steps with the simultaneous removal of the protecting group) (Scheme 3).

3.1.2. Synthesis of Analogues **7** and **9a–f**

The third class of designed analogues features modifications at the C2 position.

Our initial synthetic strategy for these compounds involved performing a direct arylation or Suzuki coupling on an advanced precursor utilising iodide **1** and trimethylsylyl acetylene **29** in the Larock cyclisation [13,34] (Scheme 5). However, this transformation did not yield the desired benzofuran derivative **30** but instead produced its open and irrelevant structural isomer.

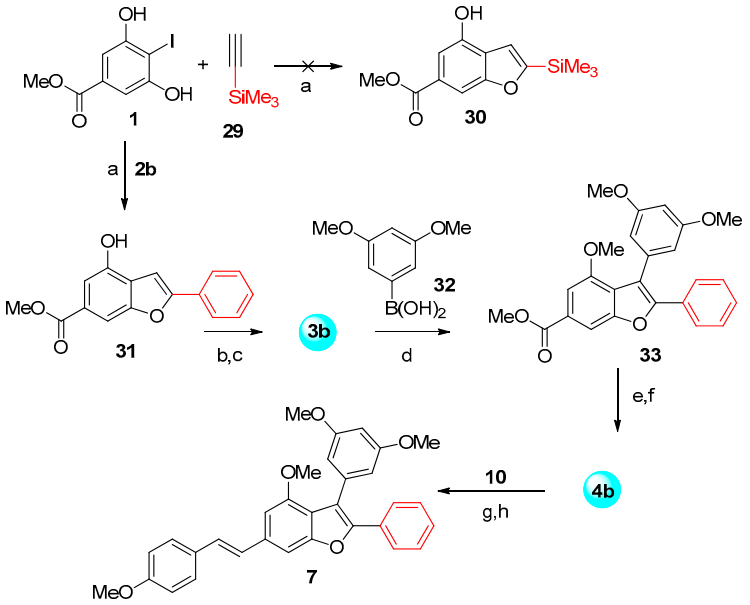

Scheme 5. (a) **2b** or **29**, $PdCl_2(PPh_3)_2$, CuI, Et_3N, 80 °C, 85% for **31**; (b) MeI, K_2CO_3, acetone, quant.; (c) NIS, TFA, CH_3CN, 45%; (d) **32**, $PdCl_2(PPh_3)_2$, $NaHCO_3$, DMF/H_2O (4:1), 75%; (e) DIBAL-H, DCM; (f) DMP, DCM; 80% in two steps; (g) **10**, LiOH, LiBr, i-PrOH, reflux; (h) I_2 cat., n-heptane: DCM (7:3), 64% in two steps.

Nevertheless, to understand the influence of the *para*-methoxy group of the C2 aryl ring on PAA's biological activity, we decided to follow the complete sequence of reactions used for PAA's synthesis to prepare the analogue **7** bearing a simple phenyl ring. Indeed, iodide **1** [9] was used in the domino Sonogashira-hetero-annulation reaction with phenylacetylene **2b,** affording the desired benzofuran **31** in a good yield (85%).

Quantitative methylation followed by iodination produced **3b** (Scheme 5), which was then used in the Suzuki reaction with boronic acid **32** to furnish the cross-coupled product **33** in a 75% yield. This product, reduced to aldehyde **4b**, was used in the Wittig olefination and isomerisation with the standard conditions to afford compound **7** in an overall good yield (Scheme 5).

Finally, to investigate the effect of the substituents at the C-3 position, we prepared analogues with different aryl moieties at C-3 (compounds **9a**–**f**). The synthesis of these analogues was performed using the intermediate iodide **8** in Suzuki cross-coupling reactions with variously substituted aryl boronic acids (Scheme 6).

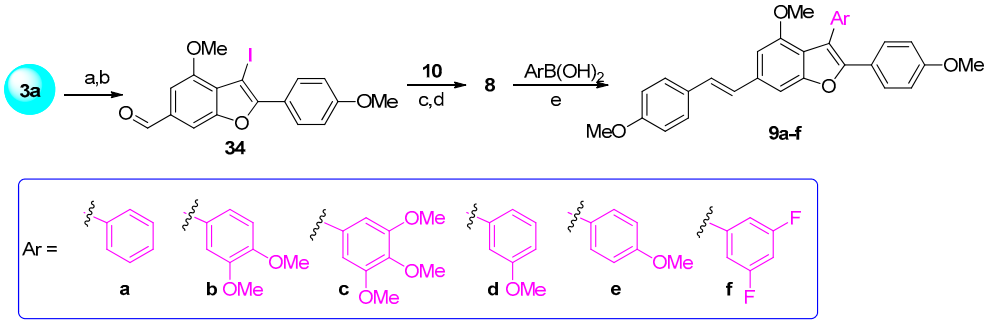

Scheme 6. (a) DIBAL-H, DCM, 0 °C, 24 h; (b) DMP, DCM, rt, 90% in two steps; (c) **10**, LiOH, LiBr, *i*-PrOH, reflux; (d) I_2 cat., *n*-heptane: DCM (7:3), 66% in two steps; (e) $ArB(OH)_2$, $PdCl_2(PPh_3)_2$, $NaHCO_3$, DMF/H_2O (4:1), 80 °C, 56–86% for **9a**–**f**.

Intermediate **8** was prepared starting from iodide **3a** [9], which was chemoselectively reduced to the benzylic alcohol by DIBAL-H and then oxidised by DMP to the corresponding aldehyde **34** (90% yield over two steps). The usual Wittig reaction with

phosphonium salt **10** furnished the *trans* isomer **8** (66% yield) after the isomerisation of the resulting *cis*/*trans* mixture. In the final step, compounds **9a–f** were obtained through Suzuki reactions, introducing either a phenyl (**9a**), a 3,4-dimethoxybenzene (**9b**), a 3,4,5-trimethoxybenzene (**9c**), a 3-methoxybenzene (**9d**), a 4-methoxybenzene (**9e**), or a 3,5-difluorobenzene (**9f**) group at the C3-position of compound **8** in 56-86% yields.

3.2. Antiproliferative Effect of the 13 Analogues Compared to PAA

3.2.1. Antiproliferative Effect on HepG2 Cells

After their synthesis and purity determination by NMR spectroscopy (>99%), the antiproliferative effect of the PAA derivatives was evaluated on the hepatocellular carcinoma HepG2 cell line using the MTT assay. To this end, HepG2 cells were exposed to a broad spectrum of concentrations, ranging from 10 nM to 100 µM, of PAA or PAA analogues for 72 h. Among the thirteen new compounds tested, only compounds **9a** and **9f** exhibited significant cytotoxic activity against HepG2 cells (Figure 2). Specifically, analogue **9a**, which features a phenyl ring at the C3 position, reduced cell viability by approximately 50% at concentrations of 10 µM and 100 µM, although this effect was less pronounced than that of PAA (Figure 2). In contrast, compound **9f**, which has fluorine atoms on the C3 aryl ring, showed a variable response, with a slightly proliferative effect at a 10 nM concentration and a cytotoxic activity of about 30% at the highest concentration tested. The other PAA analogues did not demonstrate significant antiproliferative effects up to 100 µM (Figure 2). Since all these new compounds were less active or completely inactive than PAA, assays on healthy cells were not performed.

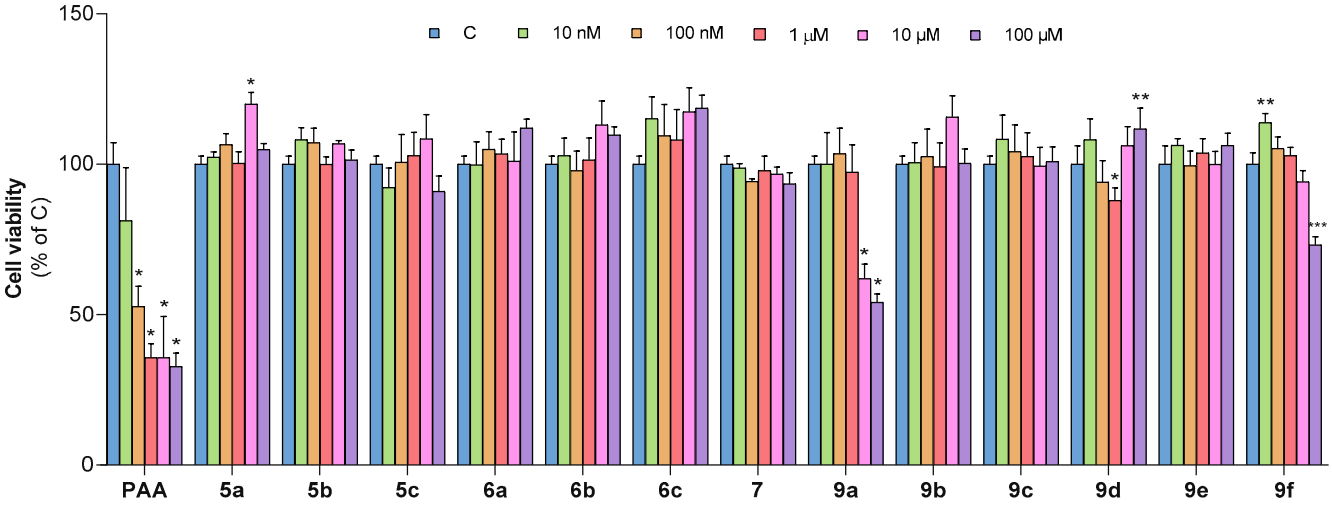

Figure 2. Antiproliferative effects of PAA and derivatives **5a–c**, **6a–c**, **7**, and **9a–f**. HepG2 cells were treated with DMSO (C), PAA, or PAA derivatives at the indicated concentrations (10 nM, 100 nM, 1 µM, 10 µM, and 100 µM). Cell viability was assessed after 72 h exposure by MTT assay. Data are expressed as mean ± SD of three independent experiments with four replicates. Where indicated, differences were significant according to one-way ANOVA followed by Dunnett's multiple comparison test (* $p < 0.05$, ** $p < 0.001$, *** $p < 0.001$).

3.2.2. Antiproliferative Effect on Alexander Cells

We also tested the most active analogues, **9a** and **9f,** against the Alexander cell line, which consists of epithelial cells isolated from the liver of a donor with hepatoma. The cytotoxic activity of **9a** and **9f**, along with PAA used as a reference, was assessed using the MTT assay at different concentrations (ranging from 10 nM to 100 µM), as illustrated in Figure 3.

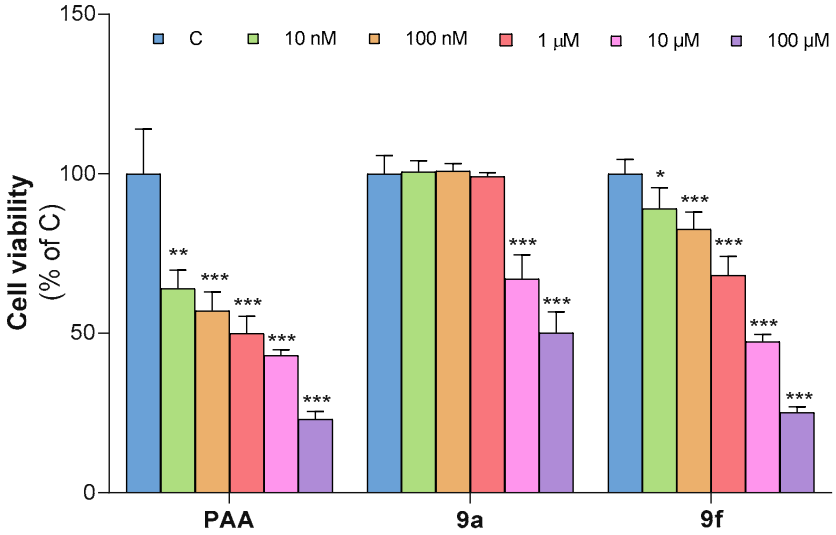

Figure 3. Antiproliferative effects of PAA and derivatives **9a** and **9f**. Alexander cells were treated with DMSO (C), PAA, or PAA derivatives at the indicated concentrations (10 nM, 100 nM, 1 μM, 10 μM, and 100 μM). Cell viability was assessed after 72 h exposure by MTT assay. Data are expressed as mean ± SD of three independent experiments with four replicates in each. Where indicated, differences were significant according to one-way ANOVA followed by Dunnett's multiple comparison test (* $p < 0.05$, ** $p < 0.001$, *** $p < 0.001$).

Interestingly, both **9a** and **9f** exhibited cytotoxic activity against the Alexander cells but in different ways. Specifically, **9a** was active only at the higher concentrations of 10 and 100 μM, where cell viability was reduced by about 30% and 50%, respectively. In contrast, analogue **9f** was more active than **9a**, with a 12% reduction in cell viability, starting at a concentration of 10 nM and reaching 50% and 75% reduction at 10 μM and 100 μM, respectively. However, both analogues were less active than PAA, which achieved a 40% reduction in cell viability just at the low concentration of 10 nM.

3.3. Computational Studies

3.3.1. Structure Optimisations

Computational studies were aimed at understanding the 3D structure of the PAA analogues synthesised in this article and looking for the interaction between the structure and relative electron density on the one hand and the biological activity on the other (see "Computational details" in Materials and Methods, Section 2.3, for a description of the used methods). In this regard, we decided to limit such studies to PAA, **9a** (with an unsubstituted phenyl at C-3), **9b**, and **9c** (both bearing a para-methoxy group). PAA was chosen as a reference compound due to its high antiproliferative effect. Additionally, **9a**, **9b**, and **9c** were chosen because of their different C-3 substituents and their related different biological activities. Indeed, based on our empirical results, the functionalisation of C-3 is essential to distinguish between active compounds (e.g., **9a** and **9f**) and inactive ones (**9b** and **9c**).

A graphical view of the obtained structures is shown in Figure 4. All the compounds present the benzofuran core, the styryl substituent at C-6, and the *para*-methoxyphenyl group at C-2 in a substantially coplanar arrangement. In contrast, the phenyl group at C-3 is significantly rotated relative to the rest of the molecular structure. The dihedral angle between the average planes of the benzofuran core and the C-3 phenyl group is computed to be approximately 60 degrees in all four studied compounds.

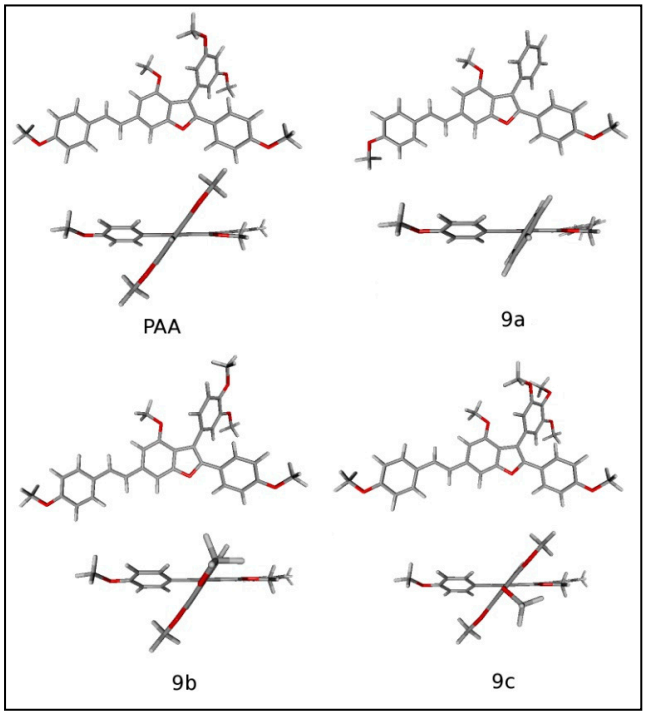

Figure 4. Computed stable conformers of PAA, **9a**, **9b**, and **9c**.

3.3.2. Conformational Study and Electronic Properties

A conformational study was performed for PAA, **9a**, **9b**, and **9c** to research alternative structures in which the phenyl group at C-3 is coplanar with the benzofuran core. These attempts did not lead to new stable conformers, suggesting a strong energetic preference for the not-planar orientation of the phenyl group at C-3. Such a preference is unaffected by the presence of the methoxy groups on this phenyl ring. The inability to arrange both the phenyl groups at C-2 and C-3 in a coplanar manner is likely due to steric strain occurring between the two rings. Hence, from our studies, we can conclude that only one phenyl group can be coplanar with the benzofuran core, and evidently, the ring at C-2 is energetically favoured.

The fact that the phenyl group at C-3 is neatly rotated in the studied compounds suggests that no significant differences should be expected in terms of conjugative effects between the benzofuran moiety and the phenyl ring when comparing PAA to **9a**–**c**.

In this respect, atomic charges for the oxygen and carbon atoms of the benzofuran core were computed in the series of studied compounds. The obtained Mulliken and natural charges (based on the NBO analysis) are reported in Table S1 of the Supporting Information. From the data, it is evident that no significant changes were observed when comparing PAA with **9a**–**c**. Indeed, it is reasonable to state that the different substitutions on the phenyl ring at C-3 do not induce significant changes in the electronic density of the remaining molecular structure.

A substantial invariance was also observed in the molecular orbitals (MOs) close to the HOMO and LUMO in terms of MO shapes and energies. Figure 5 shows the MOs calculated in PAA and **9a**–**c**. Interestingly, all the reported MOs are mainly localised on the coplanar part of the molecule, and their energy levels are in black in the figure, with the exception of one MO, which is primarily localised on the phenyl group at C-3 (the yellow level). The MO shapes are shown for PAA as an example in Figure 4.

It is evident that the first type of MO (black levels) exhibits substantial invariance in terms of orbital energy in the series of compounds. This finding is mirrored by a significant invariance in the MO shape across the series of the four compounds. In contrast, and as

expected, the MO primarily localised on the phenyl ring at C-3 (yellow levels) shows big changes in both shape and energy.

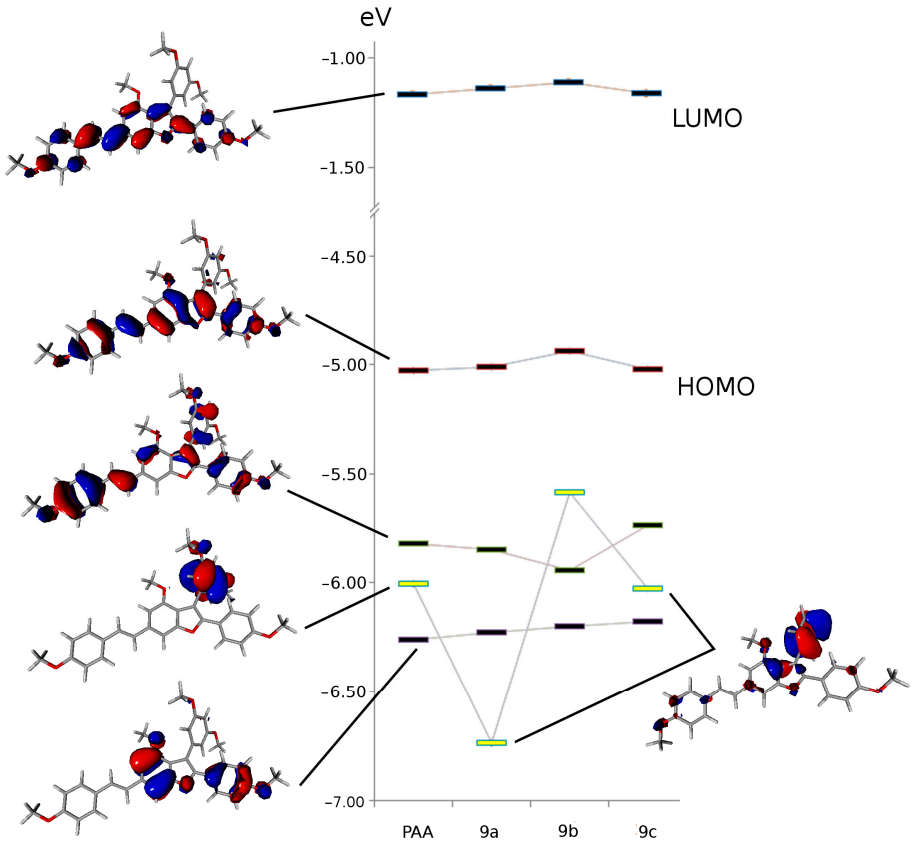

Figure 5. Selected MOs of PAA, **9a**, **9b**, and **9c,** which are close in energy to the HOMO and LUMO. The yellow levels are associated with MOs mainly localised on the phenyl group at the benzofuran C-3. The black levels refer to MOs localised on the benzofuran core and the remaining nearly coplanar groups.

3.4. Structure–Properties Relationship Conclusion

Based on the biological assays and computational studies, we can gain valuable information about the PAA biological activity. Indeed, we can assess the following:

- The *trans* configuration of the double bond is essential for the cytotoxicity of PAA, as the *cis* isomer (**5a**) and the analogues with the ethylene bridge (**5b**) or a triple bond (**5c**) were inactive.
- The presence of only one methoxy group in the *para* position on the styryl ring is important since additional methoxy substituents (as in **6b** and **6c**) or a hydroxyl group instead of the methoxy group all resulted in inactive compounds.
- The *para*-methoxy substituent on the C-2 ring is fundamental for the biological activity of PAA since its absence (as in analogue **7**) resulted in an inactive species.
- The C-3 ring is the only portion of the molecule that can be modulated to produce other active species, such as compound **9c,** with a plain unsubstituted phenyl ring, or analogue **9f,** with two fluorine atoms, even if both analogues were less active than PAA.

Moreover, through computational studies, we have learned that PAA has a rigid and planar structure, with the C-3 phenyl ring being the only exception. This ring is out of the plane with a 60° dihedral angle relative to the rest of the molecule. We also computed a conformational invariance between PAA and **9a–c** analogues, all of which have

a planar structure except for the C-3 ring, which is about 60° out of the plane, regardless of its substitution.

Due to the lack of electronic conjugation between the C-3 phenyl ring and benzofuran core, no significant changes were computed in terms of electronic density and, in general, the electronic properties of the coplanar core of the studied molecules. However, the electronic structure of the C-3 phenyl ring changes significantly from one compound to another. Therefore, the measured changes in the antiproliferative activities in the four studied compounds should be associated with the direct effects of the C-3 phenyl rather than an indirect perturbation on the rest of the molecule. In this respect, and on an empirical basis, we can highlight that the presence of the -OMe substituent in the *para* position (as in **9b** and **9c**) is completely deleterious for the desired biological activity of the PAA derivatives. The presence of two OMe groups in the *meta* positions improves the antiproliferative effect (PAA compared to **9a**) but does not seem to be strictly necessary.

Moreover, compound **9f** showed higher cytotoxic activity than **9a**, especially against the Alexander cell line. This can be explained by the similar size of hydrogen and fluorine atoms, making **9a** and **9f** structurally similar. However, the fluorine atoms, unlike hydrogen atoms, exert both inductive and mesomeric effects on the phenyl C-3 ring, resulting in a greater influence on the overall structure [35]. Due to its high electronegativity, F can affect the lipophilicity/hydrophilicity balance of the compound. Moreover, likewise to the methoxy moiety, F is a moderate hydrogen acceptor, so the two fluorines in compound **9f** interact with the biological target in a similar manner to the two methoxy groups of the C-3 ring of PAA. In the end, it can be affirmed that the phenyl C-3 ring seems to be fundamental for the antiproliferative activity [10], as well as the nature and the position of the substituents on the ring.

4. Conclusions

In summary, thirteen new PAA derivatives were synthesised by using different synthetic strategies. In vitro MTT assays were performed to evaluate the cytotoxic activity of the synthetised compounds. The biological results clearly demonstrated that the overall structure of PAA plays a critical role in cell viability. The *trans* stereochemistry of the double bond is essential for activity, as the *cis* isomer (**5a**) was inactive. Neither the extreme rigidity of the linear compound **5c** nor the flexibility of compound **5b** increased cytotoxicity. A single methoxy group on the styryl portion and one on the aryl ring at the C-2 position are essential; additional methoxy groups in compounds **6b** and **6c** or a hydroxyl group instead of methoxy in **6a** or **6c** are ineffective. Moreover, the C-3 group proved to be the only portion of the molecule that can be modulated to obtain other active compounds. In fact, only the analogues **9a**, with an unsubstituted phenyl ring at the C-3 position, and **9f**, with fluorine atoms on the same ring, showed antiproliferative activity, although this was less than PAA. In contrast, the presence of a *para* OMe group on the C-3 ring, as in analogues **9b**, **9c**, and **9e**, dropped the biological activity. The importance of the C-3 ring was also confirmed by computational studies on PAA and analogues **9a**–**c**. These studies showed that the C-3 ring is the only part of the molecule that deviates from the planar structure formed by the benzofuran and the styryl core. Furthermore, the C-3 ring exhibited electronic variance among the studied analogues, highlighting its significant role in the biological activity of PAA and PAA's analogues. Studies aimed at developing more potent and selective derivatives based on these new findings are currently ongoing in our laboratory. Different positions of fluorine, as well as different halogens or substituents (EWG as CF_3, NO_2, etc.) on the ring, will be introduced, and the results will be presented in due course.

Supplementary Materials: The following supporting information can be downloaded at: https://www.mdpi.com/article/10.3390/org5030012/s1. Procedures for the preparation of synthetical precursors and final compounds, cell culture and cell viability assays, and computational details. Copies of ^{1}H and ^{13}C NMR spectra of selected compounds were reported.

Author Contributions: Conceptualisation, L.C.; methodology, I.C., A.S. (Alessandro Santarsiere), and A.S. (Anna Santarsiero); software, M.A.; validation, P.C. and A.S. (Anna Santarsiero); investigation, I.C., A.S. (Alessandro Santarsiere), and A.S. (Anna Santarsiero); data curation, A.S. (Alessandro Santarsiere), P.C., and I.C.; writing—original draft preparation, L.C.; writing—review and editing, M.A., M.F., and P.L.; supervision, L.C.; funding acquisition, L.C. All authors have read and agreed to the published version of the manuscript.

Funding: This research received no external funding.

Conflicts of Interest: The authors declare no conflicts of interest. The funders had no role in the design of the study, in the collection, analyses, or interpretation of data, in the writing of the manuscript, or in the decision to publish the results.

References

1. Kotecha, R.; Takami, A.; Espinoza, J.L. Dietary Phytochemicals and Cancer Chemoprevention: A Review of the Clinical Evidence. *Oncotarget* **2016**, *7*, 52517–52529. [CrossRef] [PubMed]
2. Keylor, M.H.; Matsuura, B.S.; Stephenson, C.R.J. Chemistry and Biology of Resveratrol-Derived Natural Products. *Chem. Rev.* **2015**, *115*, 8976–9027. [CrossRef] [PubMed]
3. Vang, O. Resveratrol: Challenges in Analyzing Its Biological Effects. *Ann. N. Y. Acad. Sci.* **2015**, *1348*, 161–170. [CrossRef] [PubMed]
4. Bala, A.E.A.; Kollmann, A.; Ducrot, P.-H.; Majira, A.; Kerhoas, L.; Leroux, P.; Delorme, R.; Einhorn, J. Cis E-viniferin: A New Antifungal Resveratrol Dehydrodimer from *Cyphostemma crotalarioides* Roots. *J. Phytopathol.* **2000**, *148*, 29–32. [CrossRef]
5. Lin, M.; Yao, C.-S. Natural Oligostilbenes. In *Studies in Natural Products Chemistry*, 1st ed.; Atta-ur-Rahman, Ed.; Elsevier: Amsterdam, The Netherlands, 2006; Volume 33, pp. 601–644. [CrossRef]
6. Kloypan, C.; Jeenapongsa, R.; Sri-in, P.; Chanta, S.; Dokpuang, D.; Tip-pyang, S.; Surapinit, N. Stilbenoids from *Gnetum macrostachyum* Attenuate Human Platelet Aggregation and Adhesion. *Phytother. Res.* **2012**, *26*, 1564–1568. [CrossRef] [PubMed]
7. Hölscher, D.; Schneider, B. A Resveratrol Dimer from *Anigozanthos preissii* and *Musa cavendish*. *Phytochemistry* **1996**, *43*, 471–473. [CrossRef]
8. Brkljača, R.; White, J.M.; Urban, S. Phytochemical Investigation of the Constituents Derived from the Australian Plant *Macropidia fuliginosa*. *J. Nat. Prod.* **2015**, *78*, 1600–1608. [CrossRef] [PubMed]
9. Chiummiento, L.; Funicello, M.; Lopardo, M.T.; Lupattelli, P.; Choppin, S.; Colobert, F. Concise Total Synthesis of Permethylated Anigopreissin A, a New Benzofuryl Resveratrol Dimer. *Eur. J. Org. Chem.* **2012**, *2012*, 188–192. [CrossRef]
10. Convertini, P.; Tramutola, F.; Iacobazzi, V.; Lupattelli, P.; Chiummiento, L.; Infantino, V. Permethylated Anigopreissin A Inhibits Human Hepatoma Cell Proliferation by Mitochondria-Induced Apoptosis. *Chem.-Biol. Interact.* **2015**, *237*, 1–8. [CrossRef]
11. Marsico, M.; Santarsiero, A.; Pappalardo, I.; Convertini, P.; Chiummiento, L.; Sardone, A.; Di Noia, M.A.; Infantino, V.; Todisco, S. Mitochondria-Mediated Apoptosis of HCC Cells Triggered by Knockdown of Glutamate Dehydrogenase 1: Perspective for Its Inhibition through Quercetin and Permethylated Anigopreissin A. *Biomedicines* **2021**, *9*, 1664. [CrossRef]
12. Schreiber, S.L. Target-Oriented and Diversity-Oriented Organic Synthesis in Drug Discovery. *Science* **2000**, *287*, 1964–1969. [CrossRef] [PubMed]
13. Herraiz-Cobo, J.; Albericio, F.; Álvarez, M. The Larock Reaction in the Synthesis of Heterocyclic Compounds. In *Advances in Heterocyclic Chemistry*; Elsevier: Amsterdam, The Netherlands, 2015; Volume 116, pp. 1–35. [CrossRef]
14. Chao, J.; Li, H.; Cheng, K.-W.; Yu, M.-S.; Chang, R.C.-C.; Wang, M. Protective Effects of Pinostilbene, a Resveratrol Methylated Derivative, against 6-Hydroxydopamine-Induced Neurotoxicity in SH-SY5Y Cells. *J. Nutr. Biochem.* **2010**, *21*, 482–489. [CrossRef]
15. Chimento, A.; Santarsiero, A.; Iacopetta, D.; Ceramella, J.; De Luca, A.; Infantino, V.; Parisi, O.I.; Avena, P.; Bonomo, M.G.; Saturnino, C.; et al. A Phenylacetamide Resveratrol Derivative Exerts Inhibitory Effects on Breast Cancer Cell Growth. *Int. J. Mol. Sci.* **2021**, *22*, 5255. [CrossRef] [PubMed]
16. Frisch, M.J.; Trucks, G.W.; Schlegel, H.B.; Scuseria, G.E.; Robb, M.A.; Cheeseman, J.R.; Scalmani, G.; Barone, V.; Mennucci, B.; Petersson, G.A.; et al. *Gaussian 09, Revision C.01*; Gaussian, Inc.: Wallingford, CT, USA, 2010.
17. Zhao, Y.; Truhlar, D.G. The M06 Suite of Density Functionals for Main Group Thermochemistry, Thermochemical Kinetics, Noncovalent Interactions, Excited States, and Transition Elements: Two New Functionals and Systematic Testing of Four M06-Class Functionals and 12 Other Functionals. *Theor. Chem. Acc.* **2008**, *120*, 215–241. [CrossRef]
18. Ditchfield, R.; Hehre, W.J.; Pople, J.A. Self-Consistent Molecular-Orbital Methods. IX. An Extended Gaussian-Type Basis for Molecular-Orbital Studies of Organic Molecules. *J. Chem. Phys.* **1971**, *54*, 724–728. [CrossRef]
19. Dunning, T.H. Gaussian Basis Sets for Use in Correlated Molecular Calculations. I. The Atoms Boron through Neon and Hydrogen. *J. Chem. Phys.* **1989**, *90*, 1007–1023. [CrossRef]
20. Reed, A.E.; Weinstock, R.B.; Weinhold, F. Natural Population Analysis. *J. Chem. Phys.* **1985**, *83*, 735–746. [CrossRef]
21. Schaftenaar, G.; Noordik, J.H.J. Molden: A pre- and post-processing program for molecular and electronic structures. *Comput.-Aided Mol. Design* **2000**, *14*, 123–134. [CrossRef] [PubMed]
22. Antonioletti, R.; Bonadies, F.; Ciammaichella, A.; Viglianti, A. Lithium Hydroxide as Base in the Wittig Reaction. A Simple Method for Olefin Synthesis. *Tetrahedron* **2008**, *64*, 4644–4648. [CrossRef]

23. Marsh, B.J.; Carbery, D.R. One-Pot o-Nitrobenzenesulfonylhydrazide (NBSH) Formation−Diimide Alkene Reduction Protocol. *J. Org. Chem.* **2009**, *74*, 3186–3188. [CrossRef]
24. Fang, Z.; Song, Y.; Sarkar, T.; Hamel, E.; Fogler, W.E.; Agoston, G.E.; Fanwick, P.E.; Cushman, M. Stereoselective Synthesis of 3,3-Diarylacrylonitriles as Tubulin Polymerization Inhibitors. *J. Org. Chem.* **2008**, *73*, 4241–4244. [CrossRef] [PubMed]
25. Zhao, M.; Kuang, C.; Yang, Q.; Cheng, X. Cs_2CO_3-Mediated Synthesis of Terminal Alkynes from 1,1-Dibromo-1-Alkenes. *Tetrahedron Lett.* **2011**, *52*, 992–994. [CrossRef]
26. Nicolaou, K.C.; Lister, T.; Denton, R.M.; Gelin, C.F. Total Synthesis of Artochamins F, H, I, and J through Cascade Reactions. *Tetrahedron* **2008**, *64*, 4736–4757. [CrossRef] [PubMed]
27. Schechter, A.; Goldrich, D.; Chapman, J.R.; Uberheide, B.M.; Lim, D. $MgBr_2{\cdot}OEt_2$: A Lewis Acid Catalyst for the *O*- and *N*-Boc Protection of Phenols and Amines. *Synth. Commun.* **2015**, *45*, 643–650. [CrossRef]
28. Bonini, C.; Chiummiento, L.; Videtta, V. One-Pot Practical Preparation of Novel Propargylic Aryl and Heteroaryl Sulfides and Sulfones. *Synlett* **2005**, *20*, 3067–3070. [CrossRef]
29. Bonini, C.; Chiummiento, L.; Videtta, V. Direct Preparation of *Z*-1,3-Enyne Systems with a TMS-Propargylic Sulfone: Application of a One-Pot Julia Olefination. *Synlett* **2006**, *2006*, 2079–2082. [CrossRef]
30. Chankeshwara, S.V.; Chebolu, R.; Chakraborti, A.K. Organocatalytic Methods for Chemoselective *O*-*Tert*-Butoxycarbonylation of Phenols and Their Regeneration from the *O*-*t*-Boc Derivatives. *J. Org. Chem.* **2008**, *73*, 8615–8618. [CrossRef] [PubMed]
31. Rachakonda, V.; Kotapalli, S.S.; Ummanni, R.; Alla, M. Ring Functionalization and Molecular Hybridization of Quinolinyl Pyrazole: Design, Synthesis and Antimycobacterial Activity. *ChemistrySelect* **2017**, *2*, 6529–6534. [CrossRef]
32. Firouzabadi, H.; Iranpoor, N.; Ebrahimzadeh, F. Facile Conversion of Alcohols into Their Bromides and Iodides by N-Bromo and *N*-Iodosaccharins/Triphenylphosphine under Neutral Conditions. *Tetrahedron Lett.* **2006**, *47*, 1771–1775. [CrossRef]
33. Singh, S.B.; Pettit, G.R. Synthesis of (±)-Isocombretastatins A–C. *Synth. Commun.* **1987**, *17*, 877–892. [CrossRef]
34. Chiummiento, L.; D'Orsi, R.; Funicello, M.; Lupattelli, P. Last Decade of Unconventional Methodologies for the Synthesis of Substituted Benzofurans. *Molecules* **2020**, *25*, 2327. [CrossRef] [PubMed]
35. Shabir, G.; Saeed, A.; Zahid, W.; Naseer, F.; Riaz, Z.; Khalil, N.; Muneeba; Albericio, F. Chemistry and Pharmacology of Fluorinated Drugs Approved by the FDA (2016–2022). *Pharmaceuticals* **2023**, *16*, 1162. [CrossRef] [PubMed]